Inorg. Chem. **2003**, *42*, 3130–3135

$Ce_{10}Cl_4Ga_5$ and Ln_3ClGa_4 (Ln = La, Ce): Reduced Halides or Oxidized Intermetallics?

Chong Zheng,*,† HansjUrgen Mattausch,*,‡ Oliver Oeckler, and Arndt Simon

Max-Planck-Institut für Festkörperforschung, Heisenbergstrasse 1, D-70569 Stuttgart, Germany

Received October 4, 2002

The compounds $Ce_{10}Cl_4Ga_5$ and Ln_3ClGa_4 (Ln = La, Ce) were synthesized from stoichiometric mixtures of Ln, $LnCl_3$, and Ga under Ar atmosphere in sealed Ta ampules at 910–1020 °C for 25–26 days. $Ce_{10}Cl_4Ga_5$ is isostructural to $La_{10}Cl_4Ga_5$ (space group *I4/mcm*, No. 140) with lattice constants $a = 7.9546(11)$ Å, $c = 31.793(6)$ Å. Ln_3ClGa_4 represents a new structural type, also in the space group *I4/mcm*, with $a = 8.1955(8)$ and $8.1123(11)$ Å, $c = 11.363(2)$ and $11.229(2)$ Å, respectively, for Ln = La and Ce. $Ce_{10}Cl_4Ga_5$ features building blocks of Ga-centered Ce_6 trigonal prisms and distinctive two-dimensional intermetallic $CuAl_2$ and U_3Si_2 type nets. Its electronic structure falls within the realm of reduced rare-earth halides. Ln_3ClGa_4 also contains the intermetallic $CuAl_2$ type nets, but the interstitials are inverted: The building blocks are Cl-centered Ln_6 octahedra. Its electronic structure is characterized by strong peripheral Ln–Ga bonding stabilizing the Ln_6Cl octahedron which normally would have its Ln–Ln antibonding orbitals filled with electrons from interstitials beyond chalcogen. Magnetic susceptibility and conductivity measurements confirm the metallic nature of all three compounds.

Introduction

Reduced rare-earth halides are one of the most generous hosts in solid state chemistry. They can provide accommodation for very different interstitials ranging from the main group atoms H, B, Al, Ga, C, Si, Ge, N, P, As, Sb to transition metals such as Mn, Fe, Co, Ni, Ru, Os, Rh, Ir, and Pt.[1−13] Their electronic structure is characterized by the existence of "free" electrons residing in molecular orbitals centered in the rare-earth metal frameworks, hence "reducing" the rare-earth halides. For example, in La_3I_3P, a simple electron partitioning of $(La^{3+})_3(I^-)_3P^{3-}\cdot 3e^-$ leaves three electrons for three La framework atoms, or six electrons in the t_{2g} orbitals of the La_6 octahedron in the structure.[14] Adding more electrons would fill the antibonding levels of the La_6 octahedron. In fact, our attempts to synthesize Ln_3X_3Z (Ln = lanthanide, X = halogen, Z = chalcogen and halogen interstitials) of the same series have not been successful.

Intermetallic phases, on the other side, contain extensive and delocalized metal−metal bonds.[15−19] Because of the delocalized metal−metal interaction, the bonding states can span a wide range in the energy spectrum, also allowing a large selection of interstitials. Well-known examples are the Nowotny phases.[20−24] A member of these phases, the Mn_5-

* Corresponding authors.
† On leave from Department of Chemistry and Biochemistry, Northern Illinois University, DeKalb, IL 60115. E-mail: Zheng@cz.chem.niu.edu.
‡ Hj.Mattausch@fkf.mpg.de (H.M.).

(1) Simon, A.; Mattausch, Hj.; Miller, G. J.; Bauhofer, W.; Kremer, R. K. *Handbook on the Physics and Chemistry of Rare Earths;* Elsevier Science Publishers: Amsterdam, 1991; Vol. 15, pp 191−285.
(2) Mattausch, Hj.; Oeckler, O.; Simon, A. *Inorg. Chim. Acta* **1999**, *289*, 174.
(3) Mattausch, Hj.; Simon, A. *Angew. Chem.* **1998**, *110*, 498; *Angew. Chem., Int. Ed.* **1998**, *37*, 499.
(4) Warkentin, E.; Simon, A. *Rev. Chim. Miner.* **1983**, *20*, 488.
(5) Nagaki, D.; Simon, A.; Borrmann, H. *J. Less-Common Met.* **1989**, *156*, 193.
(6) Dorhout, P. K.; Payne, M. W.; Corbett, J. D. *Inorg. Chem.* **1991**, *30*, 4960.
(7) Llusar, R.; Corbett, J. D. *Inorg. Chem.* **1994**, *33*, 849.
(8) Hughbanks, T.; Rosenthal, G.; Corbett, J. D. *J. Am. Chem. Soc.* **1986**, *108*, 8289.
(9) Hughbanks, T.; Corbett, J. D. *Inorg. Chem.* **1988**, *27*, 2022.
(10) Hughbanks, T.; Corbett, J. D. *Inorg. Chem.* **1989**, *28*, 631.
(11) Mattausch, Hj.; Eger, R. Unpublished work.
(12) Meyer, G.; Wickleder, M. S. *Handbook on the Physics and Chemistry of Rare Earths*; Elsevier Science Publishers: Amsterdam, 2000; Vol. 28, chapter 177, pp 53−129.
(13) Corbett, J. D. *J. Chem. Soc., Dalton Trans.* **1996**, 575.
(14) Zheng, C.; Oeckler, O.; Mattausch, Hj.; Simon, A. *Z. Anorg. Allg. Chem.* **2001**, *627*, 2151.
(15) Kauzlarich, S. M. *Chemistry, Structure, and Bonding of Zintl Phases and Ions*; VCH: New York, 1996.
(16) Müller, U. *Anorganische Strukturchemie, 3. Aufl.*; Teubner: Stuttgart, 1996.
(17) Schäfer, H.; Eisenmann, B. *Rev. Inorg. Chem.* **1981**, *3*, 29.
(18) von Schnering, H. G. *Angew. Chem.* **1981**, *93*, 44; *Angew. Chem., Int. Ed. Engl.* **1981**, *20*, 33.
(19) Schäfer, H.; Eisenmann, B.; Müller, W. *Angew. Chem.* **1973**, *85*, 742.
(20) Jeitschko, W.; Parthé, E. *Acta Crystallogr.* **1967**, *22*, 551.

10.1021/ic026086+ CCC: $25.00
Published on Web 04/02/2003

Si_3 type compound Ln_5M_3 (Ln = lanthanide, M = main group metal), can host more than 20 different interstitials including Cr to Zn, Al, Ga, C to Pb, P to Sb, O, and Cl to I.[7,25−34]

In this contribution, we report two types of metal-rich compounds, $Ce_{10}Cl_4Ga_5$ and Ln_3ClGa_4 (Ln = La, Ce). The chemical synthesis, structure determination, computational analysis of their electronic structures, and physical property measurements are discussed.

Experimental Section

Synthesis. Ln metals (Ln = La, Ce) (sublimed, 99.99%; Alfa-Aesar, small pieces), $LnCl_3$, and Ga (99.99%; Aldrich) were used as starting materials. $LaCl_3$ was synthesized from the reaction of La_2O_3 with NH_4Cl and HCl (37% concentration). $CeCl_3$ was obtained from the reaction of Ce metal with HCl (37% concentration). The products $LaCl_3$ and $CeCl_3$ were purified twice by sublimation in a Ta tube before being used. All handling was carried out under Ar atmosphere either in a glovebox or through the Schlenk technique.

The stoichiometric mixtures (ca. 1.5 g) of the starting materials were arc sealed in Ta tubes under Ar atmosphere. The Ta tubes were then sealed inside silica glass ampules under a vacuum of ca. 10^{-2} mbar. The reaction temperatures and times were the following: $Ce_{10}Cl_4Ga_5$, 910 °C and 25 days; La_3ClGa_4, 1000 °C and 26 days; Ce_3ClGa_4, 1020 °C and 25 days. After the reactions, the ampules were opened under Ar atmosphere. Many metallic silvery thin platelike single crystals were observed in the products of $Ce_{10}Cl_4Ga_5$ and Ce_3Ga_4Cl, and for La_3Ga_4Cl, the color is golden. EDX analyses of these single crystals, using a Tescan scanning electron microscope equipped with an Oxford EDX detector, confirmed the presence of the component elements in the pertinent ratio within 10% methodical error.

Structural Determination. The reaction products were ground to fine powders under Ar atmosphere and sealed in glass capillaries for phase identification by a modified Guinier technique[35] (Cu $K\alpha_1$: $\lambda = 1.54056$ Å; internal standard Si with $a = 5.43035$ Å; Fujifilm BAS-5000 image plate system). Single crystals were transferred to glass capillaries under Na-dried paraffin oil and sealed under Ar atmosphere. They were first examined by the Buerger precession and the Weissenberg camera techniques before being characterized on a Nonius CAD4 diffractometer, a Bruker CCD or a Stoe IPDS image plate instrument. The structures were solved with direct methods using the SHELXS and SIR97 programs,[36,37] Full matrix least-squares refinement on F^2 was carried out using the SHELXTL program.[36]

All of the product compounds crystallize in tetragonal lattices of the space group *I4/mcm* (No. 140) with $Z = 4$. The crystallographic information including the fractional coordinates and selected bond lengths of these compounds is listed in Tables 1−3.

Computational Study. The molecular orbital energy levels, the density of states (DOS), and the crystal orbital overlap population (COOP)[38] curves were computed using both the tight-binding extended Hückel method (EH)[39,40] and the self-consistent linear

Table 1. Crystal Data and Structure Refinement for $Ce_{10}Cl_4Ga_5$, La_3ClGa_4, and Ce_3ClGa_4

	$Ce_{10}Cl_4Ga_5$	La_3ClGa_4	Ce_3ClGa_4
empirical formula	$Ce_{10}Cl_4Ga_5$	La_3ClGa_4	Ce_3ClGa_4
fwt	1891.60	731.06	734.69
T (K)	293(2)	293(2)	293(2)
wavelength (Å)	0.71073	0.71073	0.71073
cryst syst	tetragonal	tetragonal	tetragonal
space group	*I4/mcm* (No. 140)	*I4/mcm* (No. 140)	*I4/mcm* (No. 140)
unit cell dimensions (Å), a	7.9546(11)	8.1955(8)	8.1123(11)
c	31.793(6)	11.363(2)	11.229(2)
V (Å^3), Z	2011.7(6), 4	763.19(18), 4	738.9(2), 4
D (g/cm^3, calcd)	6.246	6.363	6.604
abs coeff (mm^{-1})	29.172	30.544	32.683
indep data/params	481/32	197/16	208/16
GOF on F^2	1.275	1.270	1.290
final R indices[a] [$I > 2\sigma I$)], R1	0.0380	0.0325	0.0355
wR2	0.1015	0.0705	0.0812
R indices (all data), R1	0.0380	0.0335	0.0359
wR2	0.1015	0.0710	0.0816

[a] $R1 = \sum||F_o| - |F_c||/\sum|F_o|$; $wR2 = [\sum[w(F_o^2 - F_c^2)^2]/\sum[w(F_o^2)^2]]^{1/2}$.

Table 2. Atomic Coordinates ($\times 10^4$) and Equivalent Isotropic Displacement Parameters (Å$^2 \times 10^3$) for $Ce_{10}Cl_4Ga_5$, La_3ClGa_4, and Ce_3ClGa_4[a]

	x	y	z	U(eq)
		$Ce_{10}Cl_4Ga_5$		
Ce(1)	6741(1)	1741(1)	4307(1)	10(1)
Ce(2)	6677(1)	1677(1)	2969(1)	13(1)
Ce(3)	5000	5000	3490(1)	14(1)
Ga(1)	3794(1)	1206(1)	3670(1)	11(1)
Ga(2)	5000	5000	2500	12(1)
Cl(1)	0	0	9449(2)	13(1)
Cl(2)	8599(5)	3599(5)	5000	19(1)
		La_3ClGa_4		
La(1)	0	0	2500	12(1)
La(2)	3390(1)	1610(1)	5000	12(1)
Ga	3568(1)	1432(1)	1992(2)	13(1)
Cl	0	0	0	17(2)
		Ce_3ClGa_4		
Ce(1)	0	0	2500	13(1)
Ce(2)	3392(1)	1609(1)	5000	13(1)
Ga	3566(1)	1434(1)	1982(1)	14(1)
Cl	0	0	0	14(1)

[a] U(eq) is defined as one-third of the trace of the orthogonalized U_{ij} tensor.

(21) Nowotny, H.; Lux, B.; Kudielka, H. *Monatsh. Chem.* **1956**, *87*, 447.
(22) Jeitschko, W.; Nowotny, H.; Benesovsky, F. *Monatsh. Chem.* **1963**, *94*, 844.
(23) Jeitschko, W.; Nowotny, H.; Benesovsky, F. *Monatsh. Chem.* **1964**, *95*, 1242.
(24) Nowotny, H.; Benesovsky, F. *Phase Stability in Metals and Alloys*; McGraw-Hill: New York, 1967; p 319.
(25) Corbett, J. D.; Garcia, E.; Guloy, A. M.; Hurng, W.-M.; Kwon, Y.-U.; Leon-Escamilla, E. A. *Chem. Mater.* **1998**, *10*, 2824.
(26) Kwon, Y.-U.; Rzeznik, M. A.; Guloy, A.; Corbett, J. D. *Chem. Mater.* **1990**, *2*, 546.
(27) Leon-Escamilla, E. A.; Corbett, J. D. *Inorg. Chem.* **2001**, *40*, 1226.
(28) Kwon, Y.-U.; Corbett, J. D. *Chem. Mater.* **1992**, *4*, 1348.
(29) Kwon, Y.-U.; Corbett, J. D. *J. Alloys Compds.* **1993**, *190*, 219.
(30) Leon-Escamilla, E. A.; Corbett, J. D. *J. Alloys Compds.* **1994**, *206*, L15.
(31) Leon-Escamilla, E. A.; Corbett, J. D. *J. Alloys Compds.* **1998**, *265*, 104.
(32) Maggard, P. A.; Corbett, J. D. *Inorg. Chem.* **2001**, *40*, 1352.
(33) Jensen, E. A.; Hoistad, L. M.; Corbett, J. D. *J. Solid State Chem.* **1999**, *144*, 175.
(34) Zheng, C.; Mattausch, Hj.; Simon, A. *J. Alloys Compds.* **2002**, *347*, 79.
(35) Simon, A. *J. Appl. Crystallogr.* **1970**, *3*, 11.
(36) Sheldrick, G. M. *SHELXTL. Version 5;* Siemens Analytical Instruments Inc.: Madison, WI, 1994.
(37) Altomare, A.; Burla, M. C.; Camalli, M.; Cascarano, G. L.; Giacovazzo, C.; Guagliardi, A.; Moliterni, A. G. G.; Polidori, G.; Spagna, R. *J. Appl. Crystallogr.* **1999**, *32*, 115.
(38) Wijeyesekera, S. D.; Hoffmann, R. *Organometallics* **1984**, *3*, 949.
(39) Whangbo, M. H.; Hoffmann, R.; Woodward, R. B. *Proc. R. Soc. London* **1979**, *A366*, 23.

Table 3. Selected Bond Lengths [Å] for for $Ce_{10}Cl_4Ga_5$, La_3ClGa_4, and Ce_3ClGa_4

	$Ce_{10}Cl_4Ga_5$[a]	
Ce(1)−Cl(1)#1	(×2)	2.9737(9)
Ce(1)−Cl(2)		3.037(4)
Ce(1)−Ga(1)#3		3.0711(18)
Ce(1)−Ga(1)	(×2)	3.1270(15)
Ce(1)−Ce(1)#4	(×2)	3.9176(17)
Ce(1)−Ce(3)	(×2)	3.9213(10)
Ce(1)−Ce(1)#6	(×3)	4.1564(7)
Ce(2)−Ga(1)	(×2)	3.2177(15)
Ce(2)−Ga(1)#3		3.2602(19)
Ce(2)−Ga(2)	(×2)	3.3159(6)
Ce(2)−Ce(3)	(×5)	3.3922(8)
Ce(2)−Ce(2)#9		3.5132(19)
Ce(2)−Ce(2)#4		3.7719(17)
Ce(2)−Ce(2)#10	(×2)	4.0029(17)
Ce(3)−Cl(1)#2		3.048(5)
Ce(3)−Ga(2)		3.1476(13)
Ce(3)−Ga(1)	(×4)	3.2177(9)
	La_3ClGa_4[b]	
La(1)−Cl	(×2)	2.8407(5)
La(1)−Ga	(×8)	3.2034(8)
La(1)−La(2)	(×2)	4.1867(5)
La(2)−Cl#1	(×2)	3.0756(5)
La(2)−Ga#3	(×2)	3.2054(18)
La(2)−Ga#5	(×4)	3.3707(16)
La(2)−Ga	(×2)	3.4237(18)
La(2)−La(2)#16		3.733(3)
Ga−Ga#5	(×2)	2.615(3)
Ga−Ga#3		2.732(3)
Ga−La(1)#3		3.2034(8)
Ga−La(2)#3		3.2055(18)
Ga−La(2)#13	(×2)	3.3707(16)
Cl−La(1)#18		2.8407(5)
Cl−La(2)#3	(×4)	3.0756(5)
La(2)−La(2)#6	(×4)	4.3495(7)
La(1)−La(2)	(×4)	4.1867(5)
	Ce_3ClGa_4[b]	
Ce(1)−Cl	(×2)	2.8072(5)
Ce(1)−Ga	(×8)	3.1720(7)
Ce(1)−Ce(2)	(×2)	4.1416(5)
Ce(2)−Cl#1	(×2)	3.0451(5)
Ce(2)−Ga#3	(×2)	3.1615(15)
Ce(2)−Ga#5	(×4)	3.3259(13)
Ce(2)−Ga	(×2)	3.3952(17)
Ce(2)−Ce(2)#16		3.6906(16)
Ga−Ga#5	(×2)	2.601(2)
Ga−Ga#3		2.709(2)
Ga−Ce(1)#3		3.1720(7)
Ga−Ce(2)#3		3.1615(15)
Ga−Ce(2)#13	(×2)	3.3259(13)
Cl−Ce(1)#18		2.8072(5)
Cl−Ce(2)#3	(×4)	3.0451(5)
Ce(2)−Ce(2)#6	(×4)	4.3064(7)
Ce(1)−Ce(2)	(×4)	4.1416(5)

[a] Symmetry transformations used to generate equivalent atoms: #1, $x + 1, -y, -1/2$; #2, $x + 1/2, y + 1/2, z - 1/2$; #3, $-y + 1, x, z$; #4, $-x + 1, -y, z$; #6, $-y + 1, x - 1, z$; #9, $-x + 3/2, -y + 1/2, -z + 1/2$; #10, $y + 1/2, -x + 1/2, -z + 1/2$. [b] Symmetry transformations used to generate equivalent atoms: #1, $-x, y, -z + 1/2$; #3, $-x + 1/2, -y + 1/2, -z + 1/2$; #5, $-y + 1/2, x - 1/2, -z + 1/2$; #6, $y, -x, z$; #13, $y + 1/2, -x + 1/2, -z + 1/2$; #16, $-x + 1, -y, -z + 1$; #18, $-x, -y, -z$.

muffin-tin orbital local density approximation method (LDA) as implemented in the Stuttgart-TB-LMTO-ASA program.[41] The electron localization function (ELF)[42−46] was also calculated using the LDA method. The standard Wigner−Seitz radii of 3.43, 2.69, and 2.84 bohr units for the La, Cl, and Ga atoms were employed in the LDF computation. The La 6p, Ga 4d, and Cl 4s and 3d states were treated as intermediate and downfoldable. Scalar relativistic equation was used together with the von Barth−Hedin local exchange-correlation potential function.[41] Approximately 200 *k*-points in the irreducible wedge of the Brillouin zone were used in the EH computation of the DOS and COOP curves. More than 1000 *k*-points in the whole Brillouin zone were generated in the LDA calculations. These *k*-points were then reduced to the irreducible wedge of the Brillouin zone. The EH parameters used in the computation are literature values[47−49] and are listed in Table 4.

Table 4. Extended Hückel Parameters

	orbital	H_{ii} (eV)	ζ_1[a]	ζ_2	c_1[a]	c_2
La	6s	−7.67	2.14			
	6p	−5.01	2.08			
	5d	−8.21	3.78	1.381	0.7765	0.4586
Cl	3s	−30.0	2.033			
	3p	−15.0	2.033			
Ga	4s	−14.58	1.77			
	4p	−6.75	1.55			

[a] Exponents and coefficients in a double ζ expansion of the d orbital.

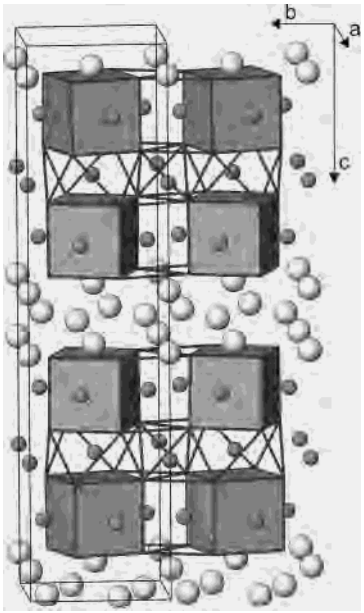

Figure 1. Perspective of the $Ce_{10}Cl_4Ga_5$ structure. The large white spheres are the Cl atoms, and the small gray spheres are the Ga atoms. The Ce_8 cubes are centered by additional Ce atoms.

Results and Discussion

Crystal Structure. $Ce_{10}Cl_4Ga_5$ is isostructural to $La_{10}Cl_4Ga_5$.[50] Its lattice features Ce-centered Ce_8 cubes connected by Ga-centered Ce_6 trigonal prisms along the ⟨100⟩ directions and by Ga-centered Ce_8 square antiprisms along *c* (Figure 1). The Cl^- ions separate these prism-based La−Ga layers. The La−Ga layers are characterized by the La (or Ga) 3^2434 and La (or Ga) 4^4 sheets in Schläfli notation. The details of the structure have been described previously.[50]

(40) Hoffmann, R. *J. Chem. Phys.* **1963**, *39*, 1397.
(41) Andersen, O. K.; Jepsen, O. *Phys. Rev. Lett.* **1984**, *53*, 2571.
(42) Faessler, T. F.; Savin, A. *Chem. Unserer Zeit* **1997**, *31*, 110.
(43) Alikhami, M. E.; Bouteiller, Y.; Silvi, B. *J. Phys. Chem.* **1996**, *100*, 16092.
(44) Becke, A. D.; Edgecomb, K. E. *J. Chem. Phys.* **1990**, *92*, 5397.
(45) Savin, A.; Nesper, R.; Wengert, S.; Faessler, T. F. *Angew. Chem.* **1997**, *109*, 1892; *Angew. Chem., Int. Ed. Engl.* **1997**, *36*, 1808.
(46) Silvi, B.; Savin, A. *Nature* **1994**, *371*, 683.
(47) Zheng, C.; Hoffmann, R. *Inorg. Chem.* **1989**, *28*, 1074.
(48) Underwoord, D. J.; Hoffmann, R.; Tatsumi, K.; Nakamura, A.; Yamamoto, Y. *J. Am. Chem. Soc.* **1985**, *107*, 5968.
(49) Canadell, E.; Eisenstein, O.; Rubio, J. *Organometallics* **1984**, *3*, 759.
(50) Zheng, C.; Simon, A.; Mattausch, Hj. *J. Alloys Compds.* **2002**, *338*, 165.

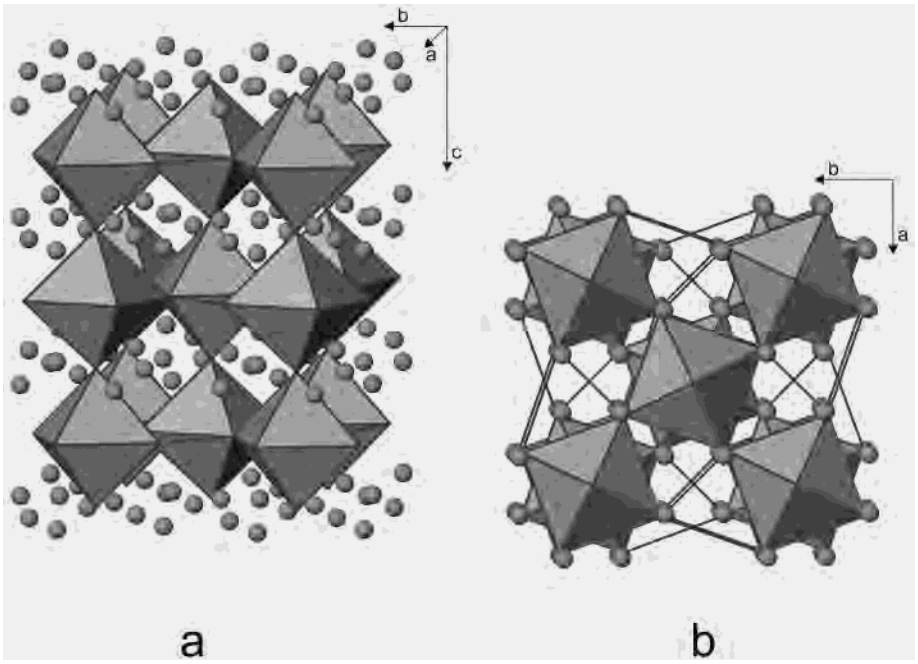

Figure 2. (a) Side view of the Ln_3ClGa_4 structure characterized by Cl-centered Ln_6Cl octahedra. The spheres are the Ga atoms. (b) Top view (along [001]) of the Ln_3ClGa_4 structure. Each Ln_6Cl octahedron is rotated by 39° with respect to the one below.

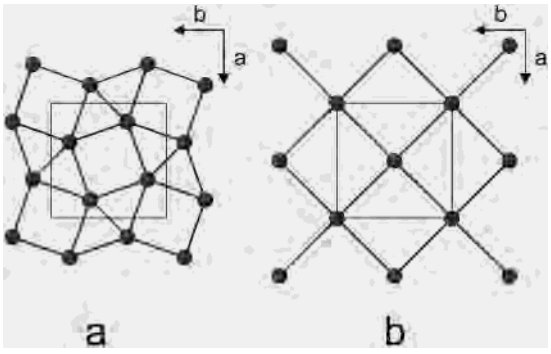

Figure 3. (a) The 3^2434 net formed the by basal Ln of the Ln_6Cl octahedra in the Ln_3ClGa_4 structure. (b) The 4^4 net formed by the apical Ln atoms of the Ln_6Cl octahedra in the Ln_3ClGa_4 structure.

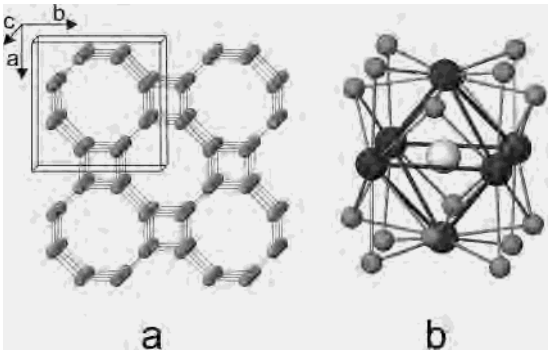

Figure 4. (a) The 48^2 nets formed by the Ga atoms in the Ln_3ClGa_4 structure stacked along the *c* direction. (b) A Ln_6Cl octahedron in the Ln_3ClGa_4 structure. The 8 faces and 8 of the 12 edges are capped by Ga atoms.

Ln_3ClGa_4 crystallizes in a new structural type. The arrangement of Ln atoms is easily described as a 3D network of corner-sharing Ln_6 octahedra each centered by a Cl atom (Figure 2). The apical atoms belong to a 4^4 net whereas the atoms in the octahedral basis, parallel to (001), form a 3^2-434 net in Schläfli notation (Figure 3). Such nets frequently occur in structures of intermetallic phases (see ref 51). In La_3ClGa_4, the La−La distance (La2−La2 in Table 3) in the octahedral basis is 4.350 Å, slightly longer than the distance between basal and apical atoms (La1−La2 in Table 3) of 4.187 Å. Ce_3ClGa_4 follows the same trend, with the Ce−Ce distances and the lattice constants slightly shorter due to the lanthanide contraction.

The 3^2434 nets are rotated by approximately 39.2° relative to each other, reminiscent of the 36° rotation found in the structure of $Ce_{10}Cl_4Ga_5$. The large voids in the $La_{6/2}Cl$ framework of Ln_3ClGa_4 are occupied by the Ga atoms, their La−Ga distances ranging from 3.203 to 3.424 Å. The Ga atoms form 48^2 nets parallel to (001), with two sets of Ga−Ga distances (Figure 4a). The one within the Ga_4 square, 2.615 Å, is shorter than the other between Ga_4 squares, 2.732 Å. Thus, each Ga atom is coordinated by three Ga atoms at distances which come near to a distance of 2.5 Å as from the single bond radius.[52] The 48^2 net is significantly puckered, the angle in the octagon is 112.8°, and that in the square is 78.8°. The sum of angles around each Ga atom is 304.6° as compared to the sum of angles around a tetrahedrally coordinated center of $3 \times 109.47 = 328.4°$. A unit cell contains two Ga 48^2 nets, each puckered toward the other with a closest approach of 4.528 Å between atoms of adjacent nets, well beyond the range for Ga−Ga bonding. The structural feature of a puckered net with covalent bonding to three neighbors corresponds to the presence of Ga^{2-}, isoelectronic to As, and within the Zintl−Klemm concept of the generalized $8 - n$ rule, La_3ClGa_4 can be formulated as a polyanionic valence compound according to $(Ln^{3+})_3Cl^-(Ga^{2-})_4$. Of

(51) Pearson, W. B. *The Crystal Chemistry and Physics of Metals and Alloys*; Wiley-Interscience: New York, 1972.

(52) Pauling, L. Die Natur der chemischen Bindung; Verlag Chemie GmbH: Weinheim, 1973.

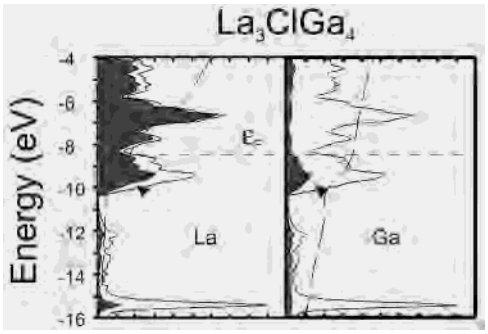

Figure 5. EH DOS plot for La_3ClGa_4. The solid line is the total DOS, the dashed line is the integrated DOS, and the shaded area is the contribution from the component indicated in the panel. The horizontal dashed line indicates the Fermi level.

course, this strict formulation in the ionic limit hides all covalency effects and incomplete electron transfer which could even allow for some Ln−Ln bonding. In that context, it is interesting to note that the octahedral Ln_6Cl unit is surrounded by Ga atoms above edges and faces as a kind of mixture between M_6X_{12} and M_6X_8 type cluster topology (Figure 4b).

Electronic Structure. The electronic structure of $Ln_{10}Cl_4Ga_5$ has been analyzed previously.[50] It is characterized by features typical of a reduced rare-earth halide compound. Hence, we will focus on the bonding of the new Ln_3ClGa_4 structure.

Figure 5 shows the total density of states (DOS) and the contribution from the La and Ga atoms, calculated by the EH method for La_3ClGa_4. The Cl s state is low in energy and thus not included in the plot. The lowest peak around −15 eV is the Cl p orbital. Continuing up in energy is the Ga s state, smeared between −16 and −11 eV. The states between −10 eV and the Fermi level are a mixture of Ga and La states. Around the Fermi level, the majority states are La d orbitals, but there is significant mixing with the Ga p state. Figure 6 presents the COOP curves for some representative bonds in La_3ClGa_4, computed by the EH method. It can be seen that, below the Fermi level, many states contribute to bonding due to the strong mixing between the La and Ga states. The dominating interactions are the short La−Cl, La−Ga, and Ga−Ga contacts, as indicated by the overlap population values integrated to the Fermi level shown in the graphs. The La−La interaction is only secondary because of the large La−La distances, yet the La−La interaction is stabilizing, contributing to positive COOP values. The significant amount of La states below the Fermi level as shown in Figure 5 suggests rather incomplete electron transfer to the surrounding Ga atoms. The LDA calculations showed similar trend.

The question of whether Ga has to be described as Ga^{2-} cannot be answered by the EH or the LDA methods as the computed charges strongly depend on the choice of basis set or Wigner−Seitz radii for the atoms. However, the ELF surface, calculated by the LDA method, shows significant electron density localized on the Ga atoms. Figure 7 demonstrates the ELF surface plotted for an isovalue equal to 0.8, viewed down the *b*-axis. For clarity, only Ga atoms

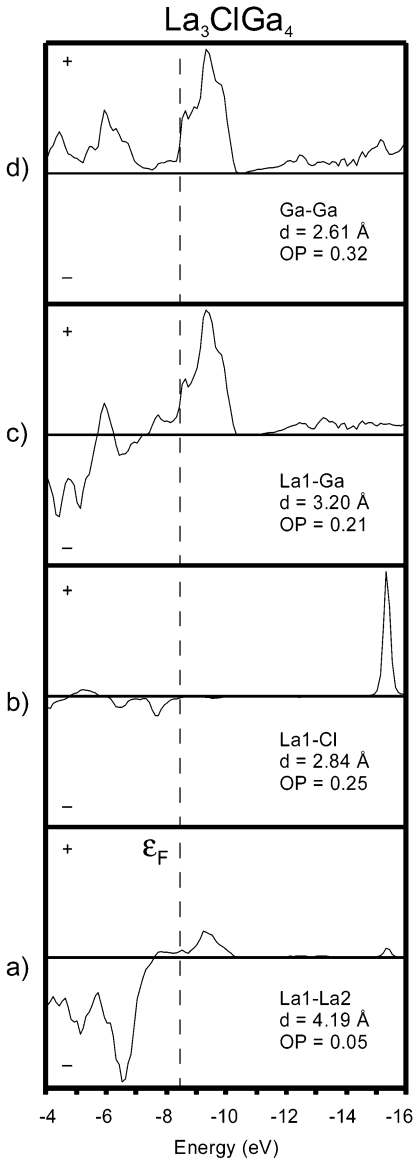

Figure 6. EH COOP plot for representative bonds in La_3ClGa_4. The + region is bonding area, and the − region is antibonding area. The bond type, its distance, and integrated overlap population to the Fermi level are indicated in the panel.

are drawn in the figure. From this figure, it is clear that a significant amount of electron density accumulates on Ga as lone pair. A decomposition of the Ga states in Figure 5 showed that a large portion of the lone pair state is localized around the −12 eV region, while the rest of the Ga state interacts with the La atoms more strongly. As is known in the EH method, the Slater orbital exponents used here were originally derived for molecular entities and are likely too diffuse for extended solid state systems. More contracted orbitals showed increase localization of the Ga lone pair state in our calculations.

If we started the bonding analysis using the cluster model shown in Figure 4b, we would arrive at a molecular orbital diagram with several energy states around the Fermi level that are of Ln−Ln bonding. These states are mixtures of La d and Ga p orbitals and can accommodate a number of electrons. This is in contrast to a normal octahedral cluster

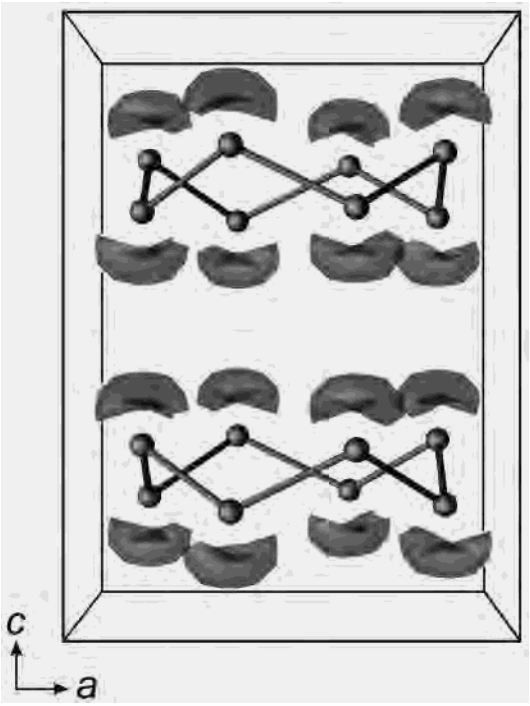

Figure 7. ELF surface at isovalue of 0.8, computed by the LDA method. For clarity, only Ga atoms are drawn.

compound for which only a t_{2g} set is usually available for Ln−Ln bonding interaction, limiting the number of skeleton electrons to 14 or 16. Nonetheless, since the primary interaction in our compounds is between the Ln atoms and halogens, we can classify these compounds as reduced halide systems. The metal−metal interaction, especially that between Ln species, is only secondary. The electron-precise nature of these compounds also supports our argument.

Physical Properties. The magnetic susceptibility of $Ce_{10}Cl_4Ga_5$ as a function of temperature in the range 5−330 K exhibits a Curie−Weiss behavior down to 150 K with a progressive bending down in $1/\chi$ versus T plot due to the (distorted octahedral) crystal field effects. The linear, high temperature part of the data was extrapolated to $\Theta = -28$ K and yielded a magnetic moment of $\mu_{eff} = 2.5\ \beta$, close to the literature value of 2.4 β for a Ce^{3+} configuration.[53] The susceptibility of Ce_3ClGa_4 is similar. Both $La_{10}X_4Ga_5$ (X = Cl, Br) and La_3ClGa_4 showed temperature-independent Pauli paramagnetism. The resistivity of La_3ClGa_4 measured in the temperature range 5−300 K shows a metallic behavior in Figure 8. This corroborates the DOS and band structure features in that there is strong La−Ga mixing, large band dispersion at the Fermi level, and incomplete electron transfer, as a complete electron transfer would result in a closed-shell electron configuration and a semiconductor. It should also be noted that the conductivity was measured for pressed power pellets. Single crystals would likely show conductivity anisotropy, as the band structures calculated by both the EH and the LMTO methods demonstrate larger dispersion in the *ab*-plane than along the *c*-axis.

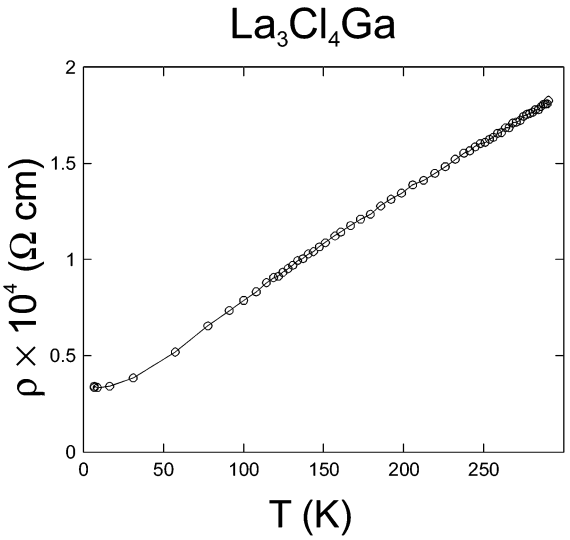

Figure 8. Resistivity of La_3ClGa_4 measured in the temperature range 5−300 K.

Acknowledgment. We thank V. Duppel for the EDX measurements, C. Kamella for the drawing of the figures, E. Brücher for the magnetic susceptibility measurements, and G. Siegle for the conductivity measurements. C.Z. acknowledges the support by NSF through Grants DMR-9704048 and CHE-9974760, and by the Max-Planck-Gesellschaft which made his visit at MPI possible.

Supporting Information Available: Listing of X-ray crystallographic details in CIF format. This material is available free of charge via the Internet at http://pubs.acs.org.

IC026086+

(53) van Vleck, J. H. The Theory of Electric and Magnetic Susceptibilities; Oxford University Press: London, 1965.